

ARTICLE

Simvastatin Induces Delayed Apoptosis Through Disruption of Glycolysis and Mitochondrial Impairment in Neuroblastoma Cells

Crystal L. Kuzyk^{1,†}, Colin C. Anderson^{1,†} and James R. Roede^{1,*}

Simvastatin, a commonly used cholesterol-lowering drug, inhibits the mevalonate pathway involved in the synthesis of the mitochondrial electron carrier coenzyme Q10 (CoQ10), as well as other bioenergetics substrates. The purpose of this study was to investigate simvastatin exposure on mitochondrial respiration, metabolic fuel preferences, and glucose utilization. We hypothesized that simvastatin at a noncytotoxic dose will impair energy metabolism in human neuroblastoma cells. SK-N-AS cells were exposed at acute and chronic time points and evaluated in a Seahorse XF analyzer, revealing decreased mitochondrial and glycolytic parameters. Flow cytometry showed a significant induction of apoptosis in simvastatin-treated cells at 48 hours. Finally, multiple techniques were used to show that simvastatin-mediated impairment of bioenergetics is more complex than CoQ10 depletion or hampered glucose uptake. Therefore, the data reported here represent a biphasic hit to mitochondria followed by reduction in glucose and glutamine metabolism in neuroblastoma; adding mechanism to potential pleotropic effects of statins.

Study Highlights

WHAT IS THE CURRENT KNOWLEDGE ON THE TOPIC?

✓ Statin therapeutics are commonly prescribed for the control and maintenance of cholesterol levels within the body. Recently, these compounds have been associated with both negative adverse effects on skeletal muscle and potential pleotropic effects, such as antitumorigenic properties in cancer and neuroprotection. The underlying mechanisms of these off-target effects are still widely unknown, yet research has pointed to mitochondrial dysfunction as a major hallmark in statin toxicity.

WHAT QUESTION DID THIS STUDY ADDRESS?

✓ This study addresses the underlying mechanisms and molecular targets of simvastatin, a model lipophilic statin therapeutic, as it relates to energy metabolism and apoptosis in a neuroblastoma cell line.

WHAT DOES THIS STUDY ADD TO OUR KNOWLEDGE?

✓ This study further characterizes the toxic mechanisms of simvastatin in a neuronal cancer cell line. The data presented here show distinct biphasic toxicity in this cell model, with apoptotic mechanisms related to decreased glutamine and glucose oxidation.

HOW MIGHT THIS CHANGE CLINICAL PHARMACOLOGY OR TRANSLATIONAL SCIENCE?

✓ Until better therapeutics for cholesterol maintenance are discovered, it is conceivable that statin prescriptions will remain constant or increase over the next decade. This research aims to help answer some of the unknowns about this therapy through investigation of molecular targets and mechanisms.

The commonly prescribed cholesterol-lowering medications known as statins are primarily indicated for atherosclerotic cardiovascular disease management and risk reduction.¹ Statins impact cholesterol metabolism via the inhibition of 3-hydroxy-3-methylglutaryl-coenzyme A (HMG-CoA) reductase, a rate-limiting enzyme of cholesterol biosynthesis that catalyzes the conversion of HMG-CoA to mevalonic acid in the mevalonate (MVA) pathway.² A recent, thorough review by Collins *et al.*³ reports that, among clinicians, the cause of adverse effects of statins on muscle cells are still unknown,

although much of the evidence points to alterations in mitochondria. To that end, the MVA pathway also results in the synthesis of important isoprenoids, such as farnesyl pyrophosphate (FPP) and geranylgeranyl pyrophosphate (GGPP); precursors of cholesterol and other products that regulate numerous cellular functions.⁴ Farnesylation and geranylgeranylation involves the synthesis of dolichols, used for N-glycosylation and ubiquinone (coenzyme Q10 (CoQ10)) synthesis, a component of the electron transport chain (ETC). Additionally, FPP and GGPP are necessary for

[†]These authors contributed equally to this manuscript.

¹Department of Pharmaceutical Sciences, Skaggs School of Pharmacy and Pharmaceutical Sciences, University of Colorado, Aurora, Colorado, USA. *Correspondence: James R. Roede (james.roede@cuanschutz.edu)

Received: August 19, 2019; accepted: November 25, 2019. doi:10.1111/cts.12740

adequate function of key membrane proteins, like the Rho family of guanosine triphosphatases (GTPases). The isoprenoids FPP and GGPP function by activating GTPases through prenylation, thereby facilitating their attachment to cellular membranes, and allowing for activation of signal transduction pathways.⁵ Disruption of these prenylated cellular proteins and additional downstream effects can have significant consequences in regard to apoptosis, vesicular transport, mitochondrial dynamics, and quality control.⁴⁻⁶ Collins *et al.* also report an association with diabetes in patients on long-term statin therapy, with little mechanistic insight. However, genetic variations of HMG-CoA reductase have been identified in diabetic populations.⁷ Furthermore, statins have been reported to reduce glucose uptake in cancer cells, yet further characterization of glucose utilization after statin exposure is limited.⁸

Off-target effects of statins remain observational with little mechanistic literature available in regard to molecular targets. Increasing evidence involving cell culture and animal models suggest that statins exhibit neuroprotective benefits, such as decreased incidence of progressive neurological symptoms in rats.⁹ A potential neuroprotective effect of statins in Parkinson's disease (PD) has been observed in epidemiological studies that have demonstrated a lower incidence of PD in statin users.¹⁰⁻¹³ For example, one such analysis investigating data from the US Veterans Affairs found that simvastatin use was associated with a hazard ratio (HR) of 0.51 (confidence interval 0.4-0.55; $P < 0.0001$) for newly acquired PD in individuals 5 years of age and older.¹⁰ Moreover, a recent meta-analysis found statin use was associated with a significant risk reduction (adjusted risk ratio of 0.74; 95% confidence interval 0.62-0.90; $P < 0.001$) for PD when compared with patients on nonstatin therapy.¹¹ In contrast to these findings, a large reimbursement healthcare claims database study describing healthcare use and expenditures concluded that statin use was associated with an increased risk of developing PD (odds ratio for lipophilic statins of 1.58, $P < 0.0001$).¹⁴ Last, evidence of mitochondrial involvement in neurodegenerative conditions highlights the need for investigation into the role of statins on mitochondrial function.^{15,16}

Due to the lack of investigation into statin-mediated alterations in bioenergetics, the purpose of this study was to investigate the role of lipophilic statins on mitochondrial function in the SK-N-AS human catecholaminergic neuroblastoma cell line. SK-N-AS cells possess a unique metabolic phenotype with components of dopaminergic neurons as well as the Warburg phenotype of cancer cells.¹⁷ Additionally, SK-N-AS are best suited for Seahorse XF analysis due to their better adherence and reduced dependence on serum during analysis. As many studies use SH-SY5Y neuroblastoma cells, our use of SK-N-AS will help validate the current body of research. In this study, SK-N-AS cells were exposed to acute or prolonged simvastatin and subsequently analyzed using Seahorse extracellular flux (XF) technology. The effects of simvastatin on mitochondrial oxygen consumption and ATP-generation, as well as characterization of statin-mediated alterations in mitochondrial fuel preference, were investigated. We found acute treatment with simvastatin had significant effects on oxygen consumption, whereas 24-hour treatment dampened basal respiration only. We then used a co-exposure of simvastatin

and CoQ10 to observe if supplementation would recover toxicity and found only basal respiration was partially rescued. Glycolysis was not significantly impaired by acute treatments; however, the glycolytic stress response was eliminated by a 24-hour simvastatin exposure. Additionally, we found that 50 μM simvastatin treatment induced significant apoptosis and cell death at 48 hours. These results help further define the complex mechanisms of toxicity of statin compounds, allowing for discussions on the potential use for simvastatin in other pathological spaces, like as an adjuvant therapy to traditional chemotherapeutics.

MATERIALS AND METHODS

Reagents

Chemical reagents were purchased from Sigma-Aldrich unless otherwise described.

Cell culture of SK-N-AS cells

Human, SK-N-AS neuroblastoma cells were obtained from American Type Culture Collection (Rockville, MD). They were cultured in Dulbecco's modified Eagle minimal essential medium (Life Technologies, Grand Island, NY) containing 10% fetal bovine serum (product number A316040; Gibco, Gaithersburg, MD) and 1% nonessential amino acids (Invitrogen) at 37°C under 5% CO₂.

Cell viability

For the evaluation of cell viability, SK-N-AS cells were plated in a 96-well plate (50,000 cells/well) and allowed to recover and adhere overnight. Cells were treated with simvastatin/lovastatin (0, 0.5, 1, 5, 10, 50, 150, or 500 μM ; $N = 5$) or dimethylsulfoxide (DMSO; 0.5%, $N = 5$) for 24 hours. After the treatment period, a SYTOX Green Nucleic Acid Stain (Invitrogen, PN S7020) at 0.5 μM was used to assess cell viability as per the manufacturer's protocol. A SpectraMax 190 microplate reader (Molecular Devices, Sunnyvale, CA) was used to measure fluorescence at an emission peak of 523 nm and excitation of 450-490 nm. Additionally, flow cytometry was performed on the Muse Analyzer (Millipore Sigma, Carlsbad, CA) using the Annexin V/Dead Cell Assay kit (PN MCH100105). Briefly, cells were plated in a 12-well plate at 200,000 cells per well in 1 mL culture medium. Cells were grown to ~ 80% confluence and then treated with 0.5% DMSO (Neg Ctrl; $N = 3$), 50 μM simvastatin ($N = 3$), or 10 mM H₂O₂ (Pos Ctrl; $N = 3$) for 24 hours or 48 hours. After the treatment period, cells were prepared and run according to manufacturer's protocol with samples run in triplicate with $\geq 2,000$ counts per sample.

IncuCyte analyses

Cells were plated in a 96-well plate at 50,000 cells per well in 1 mL culture medium. Cells were grown to ~ 80% confluence and then treated with 0.5% DMSO (Neg Ctrl; $N = 3$), 50 μM simvastatin ($N = 3$), or 10 mM H₂O₂ (Pos Ctrl; $N = 3$) for 24 hours. Images of SK-N-AS cells were captured before and after treatment at 10 \times magnification with the IncuCyte S3 Live Cell Analyzer (Sartorius, Ann Arbor, MI). Fluorescent probes for Caspase-3/7 activity were added prior to analysis (Cat. No. 4704) and measured as red fluorescent objects (red object count/well).

Seahorse XFp analysis

Live cell analyses of oxygen consumption (OCR) and extracellular acidification (ECAR) rates were measured with the Seahorse XF system (Agilent, Santa Clara, CA). New cell characterization was performed on SK-N-AS cells according to previously published data.¹⁸ Cells were plated at 30,000 cells per well and allowed to seed overnight in a cell culture incubator at 37°C and 5% CO₂ with an XF cartridge hydrating overnight in a non-CO₂ incubator at 37°C. On the day of the analysis, assay media was prepared similar to culture media (25 mM glucose, 1 mM sodium pyruvate, and 4 mM L-glutamine) and pH was adjusted to 7.4 ± 0.1. The XF culture plate was washed twice with assay media and a final volume of 180 µL assay media was added to cells. The XF culture plate was allowed to equilibrate in non-CO₂ incubator at 37°C for 30–60 minutes prior to assay initiation.

Acute injections

Port A on the XF cartridge is designated for acute treatment of control (0.5% DMSO) or 50 µM simvastatin at 20 µL per well. Ports BD were assigned for each stress test at varying volumes to account for injection into each well (B = 22 µL, C = 25 µL, and D = 27 µL). Simvastatin/DMSO was prepared in assay media at 10× concentration, giving a final well concentration of 50 µM.

Cell energy phenotype

Manufacturer's protocol was followed for the Cell Energy Phenotype kit with port B containing the FCCP/oligomycin stressor mix at 1.5/1.0 µM (final assay concentration).

Cell Mito stress

Manufacturer's protocol was followed for the Cell Mito Stress Test kit with port B containing oligomycin (ATP-Synthase inhibitor) at 1.0 µM, port C with 1.5 µM FCCP (mitochondrial membrane depolarizer), and port D with a mixture of 0.5 µM of each rotenone (complex I inhibitor) and antimycin A (complex III inhibitor; final well concentration).

Glycolysis stress

Manufacturer's protocol was followed for the Glycolysis Stress Test kit with port B containing 10 mM glucose, port C with 1.0 µM oligomycin, and port D with 50 mM 2-deoxyglucose (2-DG; competitive hexokinase inhibitor; final well concentration). NOTE: Assay media for this test does not include glucose or sodium pyruvate.

Fuel flex tests

Manufacturer's protocol was followed for the Fuel Flex Test kit with final well concentrations of Bis-2-(5-phenylacetamido-1,3,4-thiadiazol-2-yl)ethyl sulfide (allosteric glutamine oxidation pathway inhibitor) at 3.0 µM, etomoxir (long chain fatty acid pathway inhibitor, inhibits protein coding gene, carnitine palmitoyl-transferase 1A) at 4.0 µM, and UK5099 (inhibitor of glucose oxidation pathway, blocks mitochondrial pyruvate carrier) at 2.0 µM.

Custom CoQ10 assay

The Cell Mitochondrial Stress test was modified to include an acute injection after three baseline measurements,

followed by five measurements before initiation of the test injections. CoQ10 was prepared in a stock solution of DMSO at 100 mM and diluted in assay media to 10× concentration for acute injection.

Normalization and calculations

Each acute run was normalized to control basal ECAR or OCR (for ECAR, basal is represented after glucose injection) to account for between-run variation. For 24-hour exposures, Seahorse data were normalized to protein content. Briefly, Seahorse assay plates were centrifuged at 500 × G for 5 minutes and all but 100 µL of media was removed. Then, 10 µL of 10% SDS was added and mixed. A BCA Protein assay was performed at no dilution. CoQ10 runs were normalized to baseline measurements for each well. Figures represent parameters calculated using normalized percentage or protein-adjusted values. All calculations were made within each individual well with *N* = 7–9 representing 3 separate analyses in which significant outlier (Grubb's test) wells are removed from data analysis.

Western Blot

Approximately 20 µg of protein from cell lysate was loaded onto a 12% SDS-PAGE gel after quantitation via a BCA protein assay (Thermo Scientific, Waltham, MA). Proteins were then transferred to a nitrocellulose membrane using a Bio-Rad TransBlot Turbo (Hercules, CA). GLUT1 (Abcam, AB652), GLUT4 (Cell Signaling, 2213, Danvers, MA), and β-actin (Sigma, A5441, St. Louis, MO) primary antibodies were diluted in TBS-Tween containing 10% Super Block (Thermo Scientific, 37536) at a 1:1,000 dilution. Clarity Western ECL Substrate (Bio-Rad, 1705060) was used for imaging of the HRP secondary antibody on the ChemiDoc MP imaging system and Image Lab software (Bio-Rad). Each sample was run on two separate blots and normalized values were averaged. Images presented are representative samples of the imaged membranes.

ProQ Emerald and SYPRO Ruby gel stains

Cell lysates from previously described Western blot samples were similarly run on 12% SDS-PAGE gels and subject to the ProQ Emerald glycoprotein stain followed by the SYPRO Ruby total protein stain (Thermo Scientific, P21855) according to the manufacturer's protocol. Each sample was run on two separate blots and values were averaged.

Glucose uptake assay

A Glucose Uptake Cell-Based Assay kit was purchased from Cayman Chemical (Ann Arbor, MI, 600470) and performed on SK-N-AS cells plated at 40,000 cells per well in a 96-well plate after 24-hour exposure to DMSO or 50 µM simvastatin. The kit utilizes exposure of fluorescently tagged 2-NBDG (glucose derivative) to glucose-deprived cells over a period of time to evaluate total glucose uptake. After treatment, media was replaced with glucose-free media for 30 minutes followed by exposure to 25 mM 2-NBDG for 1–3 hours with and without 50 µM of the glucose uptake inhibitor apigenin (API). After this treatment,

plates were centrifuged @ 500 × G for 5 minutes followed by washing with Cell-Based Assay Buffer. Plates were centrifuged again, aspirated, and 100 μL of buffer was added before visualization using the Incucyte S3 instrument and 488 nm fluorescence. An analysis mask was created for SK-N-AS confluence and green fluorescence for quantitative measurements.

Statistics

All data sets were analyzed using GraphPad version 7 with either a Student’s *t*-test (with Welch’s correction where applicable) or one-way or two-way analysis of variance (ANOVA) with Bonferroni *post hoc* testing (unless otherwise noted). All Seahorse XF experiments were conducted in 2–3 plates per experiment, with 3–6 wells per treatment. **P* < 0.05, ***P* < 0.01, and ****P* < 0.001 difference from DMSO (unless otherwise noted).

RESULTS

50 μM Simvastatin is not Acutely Cytotoxic, but Shows Delayed Apoptosis at 48 Hours in Neuroblastoma Cells

To determine an appropriate concentration of simvastatin for mechanistic assessment, SK-N-AS cells were incubated with SYTOX Green Nucleic Acid Stain to assess cell death after 24-hour simvastatin and lovastatin exposure (Figure 1a). A 50 μM sublethal concentration of simvastatin was chosen for the remaining experiments due to its potency and lipophilic nature. This was confirmed by flow cytometry using Annexin V as a marker for apoptosis and 7-AAD as a dead cell stain (Figure 1b). A statistically significant but small decrease in percentage of live cells between DMSO and 50 μM simvastatin was observed

at 24 hours (DMSO = 91.7%, Simva = 87.9%), whereas 48 hours of exposure showed a greater reduction in live cells (DMSO = 90.6%, Simva = 44.1%). Morphological abnormalities were also observed in SK-N-AS cells as early as 24 hours, indicating a delayed apoptotic mechanism (Figure 1c). Real-time analysis using the IncuCyte’s phase microscope and fluorescent probes reveals a turning point in cell proliferation around 18 hours in which confluence begins to decline (Figure 1d). Although elevated at first, 50 μM simvastatin exposure does not maintain caspase-3/7 activity over 48 hours (Figure 1e).

50 μM Simvastatin Acutely Disrupts Cellular Metabolism and Mitochondrial Function

To assess the effect of simvastatin on cellular metabolism, we utilized Seahorse extracellular flux analyzer technology that can report on cellular mitochondrial and glycolytic function. To start, SK-N-AS cells were treated with 50 μM simvastatin or DMSO (0.5%) as the first Seahorse analyzer injection (port A), followed by a Cellular Energy Phenotype Assay. This assay measures real-time OCR and ECAR, which are indirect measures of mitochondrial respiration and glycolysis, respectively. These rates were measured at baseline, acute, and stressed conditions (after injection with a stressor compound mix of oligomycin and FCCP; Figure 2a). An acute injection of 50 μM simvastatin resulted in an immediate and statistically significant decrease in OCR (DMSO = 97%, Simva = 93%) and slight decrease in ECAR (DMSO = 103%, Simva = 100%) compared with DMSO (Figure 2b). From this phenotype assay, metabolic potential represents the stress response for each pathway, and is calculated by dividing the stressed OCR by the acute OCR (Figure 2c). Simvastatin impaired the cell’s ability to increase OCR to the same extent

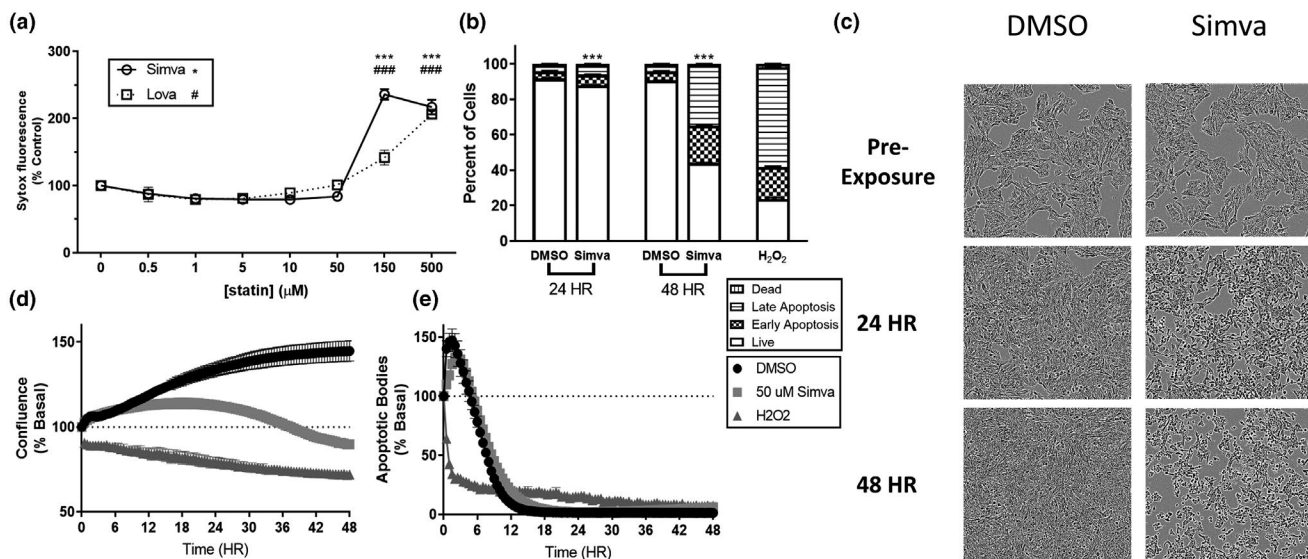


Figure 1 Fifty micromolar simvastatin induces morphological changes, cell death, and apoptosis after 24 hours of exposure in neuroblastoma cells. (a) Cell death in SK-N-AS cells plated at 50,000 cells/well in a 96-well plate after 24 hours with varying concentrations of simvastatin and lovastatin (N = 10, mean ± SEM). (b) Flow cytometry analysis after exposure to 50 μM simvastatin (N = 7–9, mean ± SEM, significance shown for live cell population). (c) Light microscopy images (10×) pretreatment and post-treatment with 50 μM simvastatin for 24 and 48 hours. Incucyte microscopic and fluorescence analysis of (d) confluence and (e) cleaved caspase-3 over 48 hours exposure (N = 5; mean ± SEM).

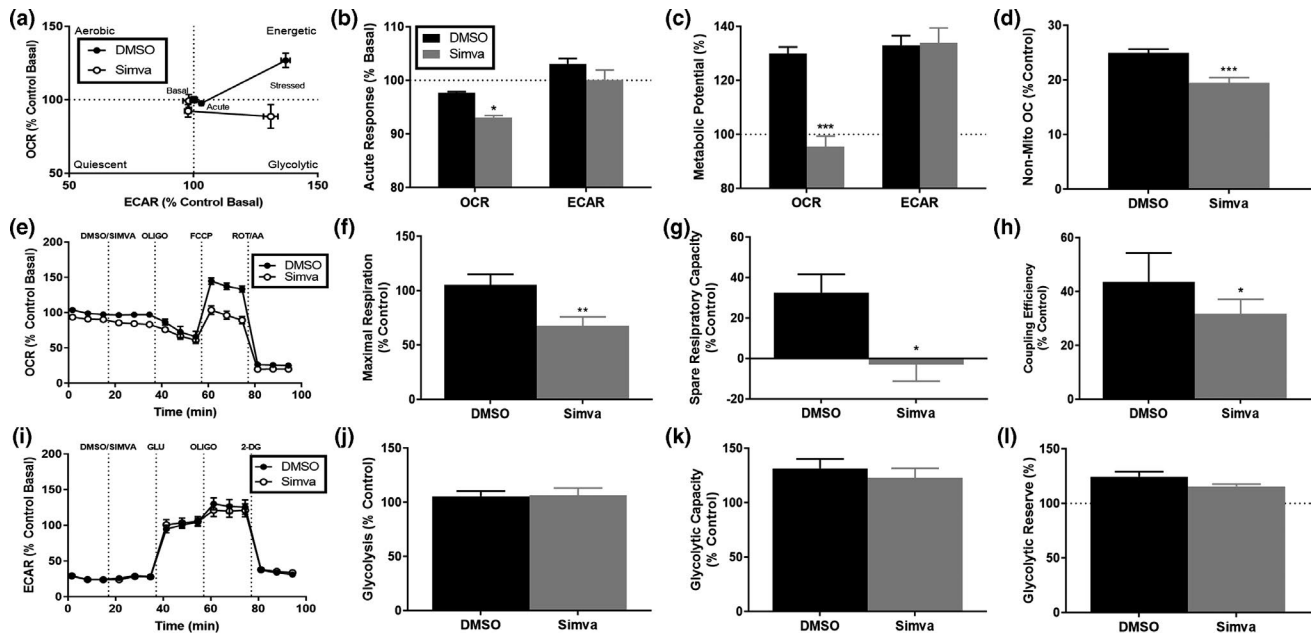


Figure 2 Fifty micromolar simvastatin causes acute disruption of mitochondrial parameters with no changes in glycolysis. (a) Tracer for the cellular energy phenotype test ($N = 7-9$, mean \pm SD). Quantification of these data seen in (b) acute response and (c) metabolic potential (mean \pm SEM). (e) Tracer for the Cell Mito Stress Test ($N = 7-9$, mean \pm SEM) with calculated individual parameters of mitochondrial function in (d) nonmitochondrial oxygen consumption, (f) maximal respiration, (g) spare respiratory capacity, and (h) coupling efficiency (mean \pm SEM). (i) Tracer for the Glycolysis Stress Test ($N = 7-9$, mean \pm SEM) with calculated individual parameters of (j) glycolysis, (k) glycolytic capacity, and (l) glycolytic reserve (mean \pm SEM). ECAR, extracellular acidification; OCR, oxygen consumption.

as the control (DMSO = 131%, Simva = 89%). These results indicate that acute treatment with simvastatin had an immediate but mild effect on glycolysis and mitochondrial respiration in addition to decreasing the ability of SK-N-AS cells to induce mitochondrial respiration in response to the stressor mix compared with control.

To follow-up on the results obtained from the phenotype assay, the Cell Mitochondrial Stress Test was used to specifically assess mitochondrial respiratory function, including basal respiration, ATP production, proton leak, and maximal respiration of simvastatin-treated neuroblastoma cells (Figure 2e). An acute injection of 50 μ M simvastatin resulted in a significant decrease in maximal respiration (DMSO = 105%, Simva = 68%; Figure 2f) and ablation of spare respiratory capacity (DMSO = 32%, Simva = -3%; Figure 2g). Additionally, decreased nonmitochondrial oxygen consumption observed in simvastatin-treated cells (DMSO = 24%, Simva = 19%; Figure 2d) may represent the reduction of alternative oxygen consuming pathways (i.e., NADPH oxidases). Coupling efficiency (DMSO = 43%, Simva = 31%; Figure 2h) was also significantly impaired in the simvastatin-treated cells compared with control, indicating less efficient mitochondria. Other mitochondrial parameters, such as ATP-linked respiration, were slightly altered in exposed cells; however, the trend was not statistically significant. These results indicate significant acute simvastatin-mediated impairments of mitochondrial function in SK-N-AS cells.

To assess the impact of acute simvastatin treatment on glycolytic ATP production, the Glycolysis Stress Test was used. The measurement of ECAR in assay media deprived of

glucose and pyruvate represents the nonglycolytic acidification rate, and is followed by a glucose injection for the basal glycolysis readings (Figure 2i). From this assay, we found that glycolysis was not significantly altered in SK-N-AS cells compared with control in the acute setting (Figure 2j-l), although the simvastatin treated cells had a trend toward a decreased glycolytic reserve.

CoQ10 Supplementation Does not Recover Acute Mitochondrial Toxicity of Simvastatin in Neuroblastoma

CoQ10 is a vital substrate synthesized from mevalonate or tyrosine for the transfer of electrons from mitochondrial ETC complexes I and II to complex III during mitochondrial respiration.¹⁹ CoQ10 has also been reported to impact plasma membrane dynamics, cell signaling, and redox chemistry as an anti-oxidant. Additionally, it has been shown that patients on long-term statin therapy have decreased blood levels of CoQ10, and CoQ10 supplementation has been recommended in a number of conditions.²⁰⁻²³ In fact, a recent review of CoQ10 supplementation references benefits in neurodegenerative diseases, as well as mitochondrial and metabolic deficiency syndromes.²⁴ To this end, many have hypothesized that the statin-mediated effects on mitochondrial respiration may be due to depletion of CoQ10. Therefore, we used the Seahorse XF system to evaluate SK-N-AS cells after an acute injection of DMSO or 50 μ M simvastatin with or without CoQ10 (Figure 3a). CoQ10 supplementation partially recovered the simvastatin-mediated decrease in basal respiration (Simva + DMSO = 56%,

Simva + CoQ10 = 68%; **Figure 3b**), nearly reaching the level of the vehicle control (DMSO + DMSO = 72%). Note, we did not previously report a decrease in basal respiration; however, these analyses allowed slightly more time (~ 10 minutes) for the simvastatin toxicity to manifest. Last, all other parameters showing simvastatin toxicity were not recovered with CoQ10 (**Figure 3c–e**).

Glycolysis is Significantly Impaired 24 Hours After 50 μ M Simvastatin Exposure, Whereas Mitochondrial Function was Recovered in SK-N-AS cells

In order to determine if simvastatin has any lasting or delayed effects on energy metabolism, we conducted Seahorse

assays after 24-hour exposure to simvastatin. To this end, SK-N-AS cells were treated for 24 hours with 50 μ M simvastatin or DMSO and subjected to the Cell Mitochondrial Stress and Glycolysis Stress tests (**Figure 4a,e**) followed by protein normalization to account for potential simvastatin-mediated changes in proliferation. The Cell Mitochondrial Stress Test indicated impaired OCR at baseline (DMSO=140 pmol/min/mg/mL, Simva=105 pmol/min/mg/mL); however, this test did not yield statistically significant differences in the other individual parameters of mitochondrial function in the other individual parameters of mitochondrial function (**Figure 4b–d,f,g**). Conversely, baseline glycolytic activity of SK-N-AS cells treated with 50 μ M simvastatin was significantly decreased nearly 50%

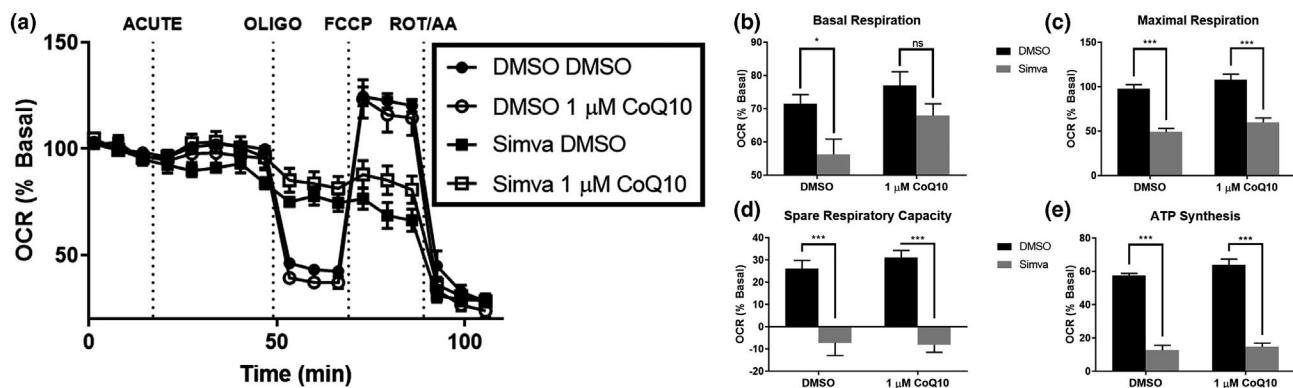


Figure 3 Coenzyme Q10 supplementation does not recover mitochondrial function after acute 50 μ M simvastatin exposure in neuroblastoma. (a) Seahorse XF Tracers ($N = 10–12$, mean \pm SEM) of a modified Cell Mitochondrial Stress test. Calculations provided by Agilent were used to measure (b) basal respiration, (c) maximal respiration, (d) spare respiratory capacity, and (e) ATP synthesis (mean \pm SEM). OCR, oxygen consumption.

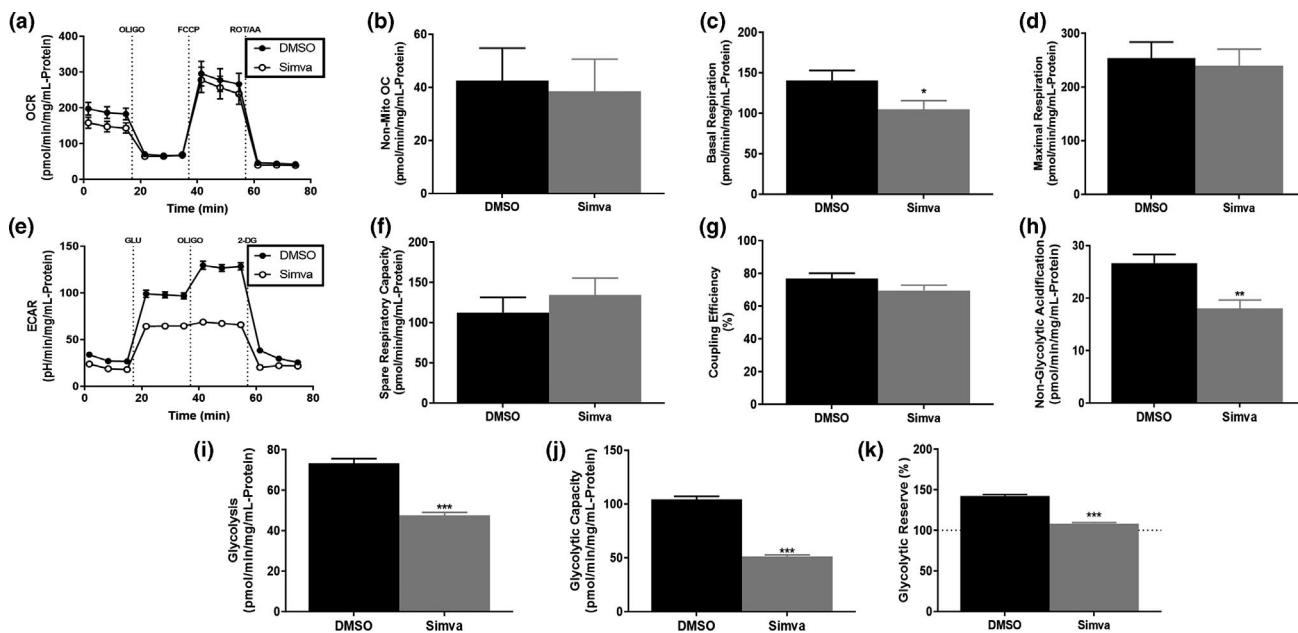


Figure 4 Neuroblastoma cells show decreases in basal mitochondrial respiration and blunted glycolysis after 24 hour exposure to 50 μ M simvastatin. (a) Tracer for the Cell Mito Stress Test ($N = 7–9$, mean \pm SEM) with calculated individual parameters of mitochondrial function in (b) nonmitochondrial oxygen consumption, (c) basal respiration, (d) maximal respiration, (f) spare respiratory capacity, and (g) coupling efficiency (mean \pm SEM). (e) Tracer for the Glycolysis Stress Test ($N = 7–9$, mean \pm SEM) with calculated individual parameters of (h) nonglycolytic acidification, (i) glycolysis, (j) glycolytic capacity, and (k) glycolytic reserve (mean \pm SEM). ECAR, extracellular acidification; OCR, oxygen consumption.

compared with control (DMSO = 73 pH/min/mg/mL, Simva = 47 pH/min/mg/mL; **Figure 4i**), leading to significant alterations in glycolytic capacity (DMSO = 104 pH/min/mg/mL, Simva = 52 pH/min/mg/mL; **Figure 4j**) and glycolytic reserve (DMSO = 143%, Simva = 109%; **Figure 4k**). Last, nonglycolytic acidification was also significantly decreased in simvastatin-exposed cells (DMSO = 26 pH/min/mg/mL, Simva = 18 pH/min/mg/mL; **Figure 4h**).

24 Hour Exposure to 50 μ M Simvastatin Diminishes Glutamine Metabolic Capacity While Increasing Dependency of Glucose and Fatty Acid Metabolism

Informed by the data from the 24-hour simvastatin treatment, we next used the Mitochondrial Fuel Flex Test to investigate the preferred fuel utilization of live SK-N-AS cells when treated with 50 μ M simvastatin or DMSO for 24 hours. Glucose, glutamine, and long-chain fatty acid (palmitate) oxidation were measured by sequential injections of fuel pathway inhibitors, as described by the assay manufacturer. Specifically, by inhibiting fuel pathways, the dependency, capacity, and flexibility of the cells to oxidize the three mitochondrial fuels can be determined. Results from these tests indicated that simvastatin-treated cells possess a significantly increased dependence on pyruvate utilization compared with control (DMSO = 45.9%, Simva = 56.6%; **Figure 5a**). Simvastatin-treated cells were found to be reliant on pyruvate oxidation as a fuel source and were unable to compensate by oxidizing other fuel sources during inhibition of the pyruvate pathway, resulting in reduced flexibility compared with control (DMSO = 6.12%, Simva = -8.3%; **Figure 5d**). Glutamine dependency was also slightly increased in simvastatin-treated cells; however, the results were not statistically significant (**Figure 5b**). Subsequently, glutamine capacity was significantly reduced in the simvastatin exposed cells (DMSO = 33.4%, Simva = 27.4%) as well as flexibility (DMSO = 20.1%, Simva = 9.6%; **Figure 5d**). Last, the

dependency of simvastatin-treated cells to oxidize fatty acids was significantly increased compared with control, indicating the cell's inability to compensate for fatty acid fuel pathway inhibition (DMSO = 48.8%, Simva = 54.9%; **Figure 5c**) leading to the elimination of fatty acid flexibility (DMSO = 11.8%, Simva = -1.2%; **Figure 5d**). The results of our fuel preference characterization tests indicate that simvastatin-mediated impairment of mitochondrial oxidative metabolism might be due to the simvastatin-mediated increase in basal dependency as well as the inhibition of metabolic stress response pathways.

Simvastatin Impairs Glucose Utilization, not Glucose Uptake in at 24 Hours in Neuroblastoma

In order to further interrogate the significant impacts of 24-hour exposure to simvastatin on glycolysis, we examined glucose uptake through investigation of the GLUT1 and GLUT4 glucose transporters, as they have been identified as primary regulators of glucose uptake that are altered in both cancer and neurodegenerative diseases.^{25,26} First, we evaluated glucose uptake using fluorescence-tagged 2-deoxyglucose (2-NBDG). Briefly, neuroblastoma cells were exposed to DMSO or 50 μ M simvastatin for 24 hours, followed by a brief 30-minute period of glucose starvation. The 2-NBDG was then supplemented into culture media and cells were exposed for 1–3 hours before washing and fluorescence measurement (**Figure 6a**). Interestingly, at all time points, cells exposed to simvastatin showed increased glucose uptake compared with the DMSO control, with the greatest effect observed at 2 hours (Simva = 162% control). To further evaluate alterations in glucose uptake, we used the glucose uptake inhibitor API as a co-exposure during 2-NBDG treatment at 50 μ M (**Figure 6b,c**). DMSO pre-treated SK-N-AS cells showed inhibition at 1 hour that is resolved at 2 hours (DMSO 1 HR = -41%, DMSO 2 HR = 8%; **Figure 6b**), whereas simvastatin-exposed cells were significantly inhibited at both 1 and 2 hours (Simva 1 HR = -66%

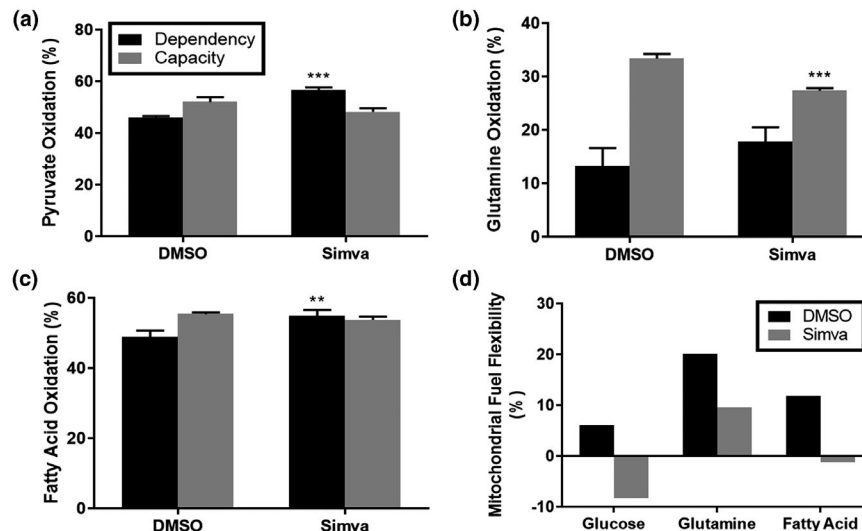


Figure 5 Fifty micromolar simvastatin impairs glutamine oxidation capacity at 24 hours, stressing all fuel sources at 24 hours. Capacity and dependency measured via the XF mitochondrial fuel flex assay for (a) pyruvate, (b) glutamine, and (c) fatty acids ($N = 7-9$, mean \pm SEM). (d) Fuel flexibility as measured by capacity average—dependency average (no error).

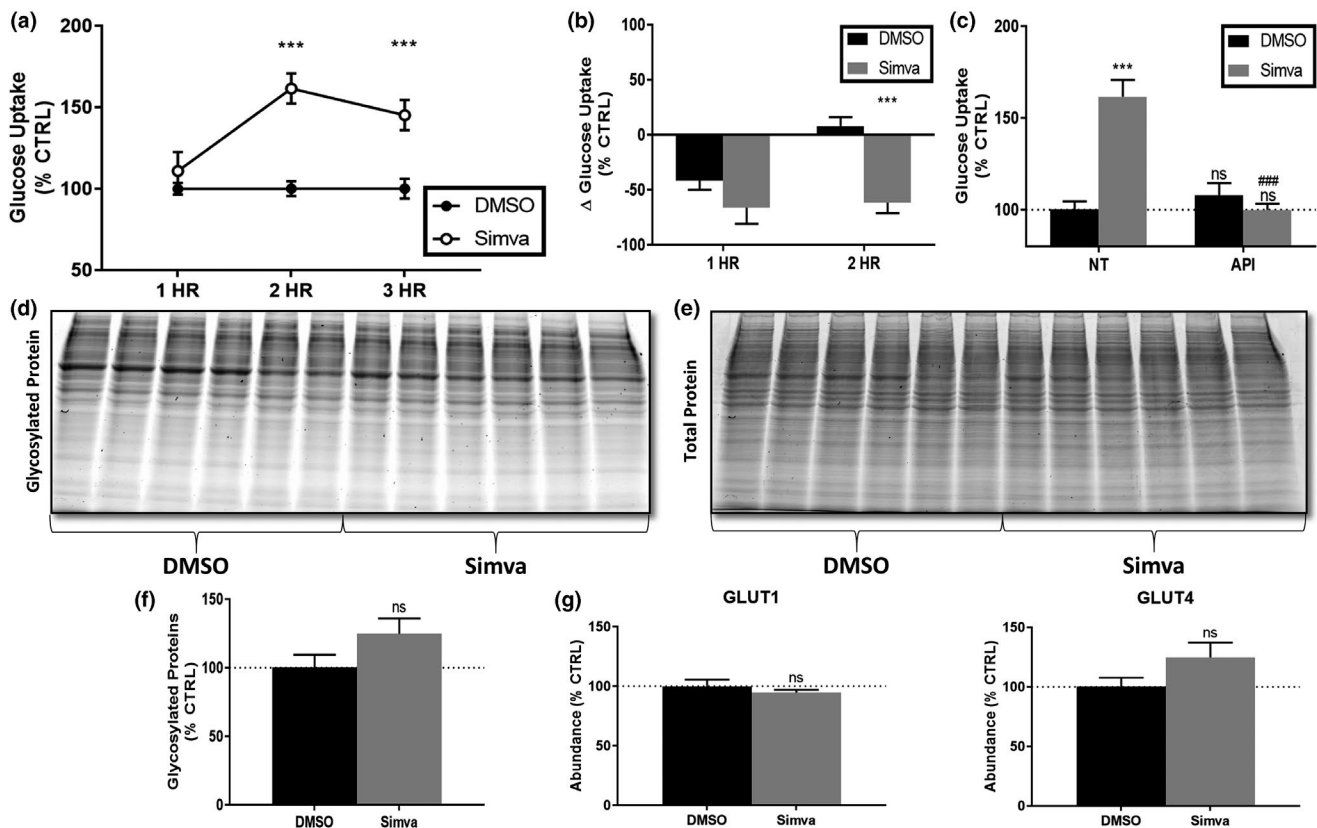


Figure 6 Simvastatin-mediated decrease in glucose metabolism is not due to altered glucose uptake in neuroblastoma. (a) Glucose uptake assay using fluorescence-labeled 2-Deoxyglucose after 24-hour exposure to 50 μ M simvastatin followed by 30 minutes of glucose starvation and 1–3 hours of exposure to 2-DG ($N = 12$, mean \pm SEM). (b) Difference of the means between no treatment (NT) and apigenin (API) treatments for 1 and 2 hour exposure to 2-DG ($N = 12$, mean \pm SEM). (c) Glucose uptake assay at the 2-hour exposure to 2-DG with addition of 50 μ M API (glucose uptake inhibitor) ($N = 12$, mean \pm SEM, # diff. from NT, all other = diff. from DMSO NT). Cell lysates after 24 hour exposures were ran on SDS-Page gels followed by the (d) ProQ Emerald glycoprotein stain and subsequently by the (e) SYPRO Ruby total protein stain. (f) Quantified glycosylated protein from gel stain experiments ($N = 6$, mean \pm SEM). (g) GLUT1 and GLUT4 protein abundance after 24 hour exposure to 50 μ M simvastatin measured by Western blot ($N = 6$, mean \pm SEM).

control, Simva 2 HR = –62% control). Moreover, DMSO-treated neuroblastoma cells showed no inhibition of glucose uptake at 2 hours, whereas simvastatin-exposed cells were inhibited back to the control treatment levels (Simva = 162% control, Simva + API = 100% control, **Figure 6c**).

Based upon the above results, we investigated claims that simvastatin-mediated disruptions in glucose metabolism are due to lack of post-translational modifications (PTMs) on GLUT1 and GLUT4 glucose transporters. Specifically, one study found that lovastatin, a compound similar to simvastatin, suppressed erythropoietin receptor activity through dual inhibition of glycosylation and geranylgeranylation of receptor protein via depletion of mevalonate pathway products, such as dolichol.²⁷ Dolichol fates are also of importance due to their potential alterations in neurodegenerative diseases like Alzheimer’s disease.²⁸ We evaluated cell lysates from SK-N-AS cells exposed to DMSO or 50 μ M simvastatin for 24 hours via SDS-PAGE followed by both the ProQ Emerald Glycoprotein gel stain and the SYPRO Ruby Total Protein gel stain (**Figure 6d,e**). Contrary to our expectations, protein glycosylation was slightly increased in simvastatin-treated neuroblastoma cells compared with control (Simva = 125% control; **Figure 6f**). Finally, we used Western blotting to

quantify the abundance of both GLUT1 and GLUT4 receptors after 24-hour simvastatin exposure (**Figure 6g**). Although a slight increase in GLUT4 abundance was observed, this alteration as not found to be statistically significant.

DISCUSSION

In the present study, our data introduce findings regarding simvastatin and its effect on mitochondrial respiration, glycolysis, and metabolic fuel preferences in neuroblastoma cells, and provides further evidence strengthening the hypothesis of dose and time-dependent cytotoxic effect of statins. Specifically, acute simvastatin treatment had a significant impact on oxidative phosphorylation and mitochondrial function in SK-N-AS cells, as well as reductions in basal mitochondrial respiration after 24-hour treatment compared with control. Results from the Cell Mitochondrial Stress Test align with previous studies reporting statin-induced mitochondrial dysfunction in different cell types.^{29,30} Due to the prevalence of statin-induced myopathies in clinical practice, the majority of previous studies focused on the skeletal muscle cells and isolated mitochondria. For example, early studies concluded that simvastatin induced cytotoxicity

in L6 rat skeletal muscle cells at concentrations between 10 and 100 μM for a period of 24 hours.²⁹ Our laboratory showed a similar effect in neuroblastoma cells at simvastatin concentrations greater than 50 μM and within 24 hours. The exact mechanisms involved in statin-induced mitochondrial dysfunction remain unknown; however, studies in isolated rat liver mitochondria have shown simvastatin-mediated inhibition of complex I, II + III, IV, and V activity at concentrations of 150 μM or more.³⁰ Other studies have suggested that inhibition of complex I leading to increased reactive oxygen species leakage and decreased ATP production may play a role in PD pathology.^{31,32} An attractive alternative hypothesis involves impaired ubiquinone production, an essential mitochondrial electron carrier of the ETC produced in the cell by products of the mevalonate pathway. A previous study in individuals treated with simvastatin reported up to a 40% decrease in serum ubiquinone concentrations.²³ Furthermore, deficiencies in CoQ10 blood levels have been observed across multiple pathologies and with aging.¹⁹ In addition, a prior study assessing mitochondrial function in neuronal cells found that prophylactic exposure to an exogenous ubiquinone compound, MitoQ, protected statin-treated cells from apoptosis.³³ Interestingly, that study concluded that the protective effect of exogenous ubiquinone was only transient, further indicating the presence of additional mechanisms of cytotoxicity. Our study reports similar observations with CoQ10 supplementation only partially recovering basal respiration, whereas the statin-mediated reduction in maximal respiration and ATP synthesis remained unchanged. Due to these observations, we can conclude that the mitochondrial toxicity of simvastatin is more than simple CoQ10 depletion via inhibition of the mevalonate pathway. Furthermore, our investigation at 24 hours shows recovered mitochondrial respiration before induction of delayed apoptosis. Although the neuroblastoma cells are metabolically stressed at 24 hours postexposure, as reported by our mitochondrial fuel flexibility analysis, they are able to maintain both basal and maximal respiration compared with control. Our 24-hour Cell Mitochondrial Stress Test data provide evidence for decreased oxidative ATP production in simvastatin-treated neuroblastoma cells; however, although the concentration of simvastatin in our study was quite lower compared with the previous studies, the supraphysiological concentrations of simvastatin used here and in other studies make it difficult to translate these findings to a potential neuroprotective effect in clinical practice.

Results of our 24-hour fuel flexibility analyses revealed an increase in pyruvate dependency and fatty acid fuel pathways. Interestingly, the reduction in glycolysis observed from the Glycolysis Stress Test did not translate to a significant decrease in pyruvate capacity; however, simvastatin-treated cells were operating at maximal glycolysis in order to maintain pyruvate oxidation. Of major significance, simvastatin exposure resulted in a significantly decreased capacity of SK-N-AS for glutamine oxidation, which has been observed to be the major reserve fuel source for this cell line.¹⁸ Alterations in glutamine utilization can impact multiple major regulatory pathways, such as glutathione production, cell growth, and proliferation.^{34,35} Furthermore, glutamine metabolism has been identified as a critically altered pathway in

cancer progression.³⁶ Reductions in pyruvate capacity may also have implications in the pentose phosphate pathway (PPP) that is believed to play a role in protecting tumorigenic cells from cell death by providing an alternative pathway for NADPH generation.³⁷ Reductions in glucose utilization can disrupt the PPP and subsequently disrupt NADPH homeostasis. The combined disruption of glucose utilization on fuel flexibility and the PPP may contribute to the cytotoxic effects of simvastatin in certain cancers. Moreover, differences in fatty acid metabolic flexibility were also observed between control and simvastatin-exposed cells. Direct inhibition of HMG-CoA reductase can lead to accumulation of acetyl-CoA in statin-treated L6 cells, which could have had an effect on fatty acid flexibility.³⁸ In addition, our data showed no statistically significant difference in fatty acid metabolic capacity between simvastatin-exposed cells and control, potentially due to accumulation of acetyl-CoA availability as an additional energy source.

Aside from statin-induced mitochondrial dysfunction, toxicity includes HMG-CoA reductase inhibition and the subsequent decreased production of MVA pathway intermediates, such as dolichol phosphate, FPP, and GGPP. FPP and GGPP are isoprenoid intermediates that activate small GTP-binding proteins involved in cell survival and maintenance through prenylation.^{39,40} Inhibition of FPP and GGPP production can have various effects on signal transduction, gene transcription, and regulation of cell growth. Of particular importance is the requirement of prenylation for certain membrane transporters for proper activity and translocation to the plasma membrane.⁴¹ As our study found decreased glucose metabolism at 24 hours, it is plausible that these reported mechanisms on the PTMs of critical membrane proteins could be associated with decreased glucose uptake. One study found that prenylated deficient Rab4 inhibits proper GLUT4 translocation to the plasma membrane, and statins have been used as prenylation inhibitors to study such mechanisms.^{42,43} Independently, dolichol phosphate deficiencies can lead to disruptions in glucose transport as well, as N-glycosylation is critical for the stable structure of GLUT1 and indirectly transport activity.⁴⁴ However, our study finds no such decrease in overall protein glycosylation, focusing our future studies on the prenylation PTM.

Glycolysis has been largely implicated in playing a role in important cellular processes involving cell survival, apoptosis, and cell death.⁴⁵ Evidence for statin-induced apoptosis exists in previous cancer studies as well, with one study finding evidence for statin-induced apoptosis driven by inhibition of Ras/mTOR signaling in hematopoietic tumor cells.⁴⁶ Additionally, previous cohort and meta-analysis studies have shown improved survival in individuals with certain types of cancer exposed to statins.^{47,48} Together, our results provide further evidence supporting that high concentrations of simvastatin exert delayed apoptosis after 24 hours in neuroblastoma cells, as well as strengthening the evidence for statin use as an adjunct therapy in the treatment of neuroblastoma. However, our study can only begin to help understand how years of statin therapy at physiological doses may offer protection from PD or impact the proliferation of cancer.

In conclusion, given the widespread use of statin therapy worldwide and increases in the aging population, it is

important to understand the molecular mechanisms associated with statin use and their clinical implications on neurological function and cancer therapeutics. As the simvastatin dose used here was supraphysiological, further studies on the pleiotropic effects of chronic statin exposure on *in vivo* cellular and metabolic parameters, and the complex mechanisms underlying these effects will provide insight into compounds created to fight cancer and neurodegenerative disease. The data reported here show distinct energetic effects of simvastatin exposure on neuroblastoma cells, providing credence to the idea that statins may sensitize neuroblastoma to other chemotherapeutics to improve their efficacy.

Funding. This research was supported by a PharmD Student Research Grant from the Associate Dean for Research, Skaggs School of Pharmacy and Pharmaceutical Sciences, University of Colorado.

Conflict of Interest. The authors declared no competing interests for this work.

Author Contributions. C.L.K., C.C.A., and J.R.R. wrote the manuscript. C.L.K. and J.R.R. designed the research. C.L.K. and C.C.A. performed the research. C.L.K., C.C.A., and J.R.R. analyzed the data.

1. Langsjoen, P.H. & Langsjoen, A.M. The clinical use of HMG CoA-reductase inhibitors and the associated depletion of coenzyme Q10. A review of animal and human publications. *BioFactors* **18**, 101–111 (2003).
2. Istvan, E.S. Structural mechanism for statin inhibition of 3-hydroxy-3-methylglutaryl coenzyme A reductase. *Am. Heart J.* **144** (6 suppl.), S27–S32 (2002).
3. Collins, R. et al. Interpretation of the evidence for the efficacy and safety of statin therapy. *Lancet* **388**, 2532–2561 (2016).
4. Willey, J.Z. & Elkind, M.S. 3-Hydroxy-3-methylglutaryl-coenzyme A reductase inhibitors in the treatment of central nervous system diseases. *Arch. Neurol.* **67**, 1062–1067 (2010).
5. Moutinho, M., Nunes, M.J. & Rodrigues, E. The mevalonate pathway in neurons: it's not just about cholesterol. *Exp. Cell Res.* **360**, 55–60 (2017).
6. Leites, E.P. & Morais, V.A. Mitochondrial quality control pathways: PINK1 acts as a gatekeeper. *Biochem. Biophys. Res. Commun.* **500**, 45–50 (2018).
7. Swerdlow, D.I. et al. HMG-coenzyme A reductase inhibition, type 2 diabetes, and bodyweight: evidence from genetic analysis and randomised trials. *Lancet* **385**, 351–361 (2015).
8. Malenda, A. et al. Statins impair glucose uptake in tumor cells. *Neoplasia* **14**, 311–323 (2012).
9. Kumar, A. et al. Neuroprotective potential of atorvastatin and simvastatin (HMG-CoA reductase inhibitors) against 6-hydroxydopamine (6-OHDA) induced Parkinson-like symptoms. *Brain Res.* **1471**, 13–22 (2012).
10. Wolozin, B. et al. Simvastatin is associated with a reduced incidence of dementia and Parkinson's disease. *BMC Med.* **5**, 20 (2007).
11. Wahner, A.D. et al. Statin use and the risk of Parkinson disease. *Neurology* **70** (16 Pt 2), 1418–1422 (2008).
12. Sheng, Z., Jia, X. & Kang, M. Statin use and risk of Parkinson's disease: a meta-analysis. *Behav. Brain Res.* **309**, 29–34 (2016).
13. Mohammad, S. et al. Pleiotropic effects of statins: untapped potential for statin pharmacotherapy. *Curr. Vasc. Pharmacol.* **17**, 239–261 (2019).
14. Liu, G. et al. Statins may facilitate Parkinson's disease: insight gained from a large, national claims database. *Mov. Disord.* **32**, 913–917 (2017).
15. Schultz, B.G., Patten, D.K. & Berlau, D.J. The role of statins in both cognitive impairment and protection against dementia: a tale of two mechanisms. *Transl. Neurodegener.* **7**, 5 (2018).
16. Murphy, M.P. & Hartley, R.C. Mitochondria as a therapeutic target for common pathologies. *Nat. Rev. Drug Discov.* **17**, 865–886 (2018).
17. Xie, H.R., Hu, L.S. & Li, G.Y. SH-SY5Y human neuroblastoma cell line: in vitro cell model of dopaminergic neurons in Parkinson's disease. *Chin. Med. J.* **123**, 1086–1092 (2010).
18. Anderson, C.C. et al. Acute maneb exposure significantly alters both glycolysis and mitochondrial function in neuroblastoma cells. *Toxicol. Sci.* **165**, 61–73 (2018).
19. Crane, F.L. Biochemical functions of coenzyme Q10. *J. Am. Coll. Nutr.* **20**, 591–598 (2001).
20. Emami, A. & Bazargani-Gilani, B. Effect of oral CoQ10 supplementation along with precooling strategy on cellular response to oxidative stress in elite swimmers. *Food Funct.* **9**, 4384–4393 (2018).

21. Zahedi, H. et al. Effects of CoQ10 supplementation on lipid profiles and glycemic control in patients with type 2 diabetes: a randomized, double blind, placebo-controlled trial. *J. Diabetes Metab. Disord.* **13**, 81 (2014).
22. Zeng, Z. et al. Efficacy of CoQ10 as supplementation for migraine: a meta-analysis. *Acta Neurol. Scand.* **139**, 284–293 (2019).
23. Rundek, T. et al. Atorvastatin decreases the coenzyme Q10 level in the blood of patients at risk for cardiovascular disease and stroke. *Arch. Neurol.* **61**, 889–892 (2004).
24. Hernandez-Camacho, J.D. et al. Coenzyme Q10 supplementation in aging and disease. *Front. Physiol.* **9**, 44 (2018).
25. Ancey, P.B., Contat, C. & Meylan, E. Glucose transporters in cancer – from tumor cells to the tumor microenvironment. *FEBS J.* **285**, 2926–2943 (2018).
26. Firbank, M.J. et al. Cerebral glucose metabolism and cognition in newly diagnosed Parkinson's disease: ICICLE-PD study. *J. Neurol. Neurosurg. Psychiatry* **88**, 310–316 (2017).
27. Hamadmad, S.N. & Hohl, R.J. Lovastatin suppresses erythropoietin receptor surface expression through dual inhibition of glycosylation and geranylgeranylation. *Biochem. Pharmacol.* **74**, 590–600 (2007).
28. Schedin-Weiss, S., Winblad, B. & Tjernberg, L.O. The role of protein glycosylation in Alzheimer disease. *FEBS J.* **281**, 46–62 (2014).
29. Kaufmann, P. et al. Toxicity of statins on rat skeletal muscle mitochondria. *Cell. Mol. Life Sci.* **63**, 2415–2425 (2006).
30. Nadanaciva, S. et al. Mitochondrial impairment by PPAR agonists and statins identified via immunocaptured OXPHOS complex activities and respiration. *Toxicol. Appl. Pharmacol.* **223**, 277–287 (2007).
31. Hu, Q. & Wang, G. Mitochondrial dysfunction in Parkinson's disease. *Transl. Neurodegener.* **5**, 14 (2016).
32. Lismont, C. et al. Redox interplay between mitochondria and peroxisomes. *Front. Cell Dev. Biol.* **3**, 35 (2015).
33. Marcuzzi, A. et al. Neuronal dysfunction associated with cholesterol deregulation. *Int. J. Mol. Sci.* **19**, 1523 (2018).
34. Burrin, D.G. & Stoll, B. Metabolic fate and function of dietary glutamate in the gut. *Am. J. Clin. Nutr.* **90**, 850S–856S (2009).
35. DeBerardinis, R.J. & Cheng, T. Q's next: the diverse functions of glutamine in metabolism, cell biology and cancer. *Oncogene* **29**, 313–324 (2010).
36. Cluntun, A.A. et al. Glutamine metabolism in cancer: understanding the heterogeneity. *Trends Cancer* **3**, 169–180 (2017).
37. Patra, K.C. & Hay, N. The pentose phosphate pathway and cancer. *Trends Biochem. Sci.* **39**, 347–354 (2014).
38. Kain, V. et al. Simvastatin may induce insulin resistance through a novel fatty acid mediated cholesterol independent mechanism. *Sci. Rep.* **5**, 13823 (2015).
39. Thompson, P.D., Clarkson, P. & Karas, R.H. Statin-associated myopathy. *JAMA* **289**, 1681–1690 (2003).
40. Buhaescu, I. & Izzedine, H. Mevalonate pathway: a review of clinical and therapeutic implications. *Clin. Biochem.* **40**, 575–584 (2007).
41. Watson, R.T., Kanzaki, M. & Pessin, J.E. Regulated membrane trafficking of the insulin-responsive glucose transporter 4 in adipocytes. *Endocr. Rev.* **25**, 177–204 (2004).
42. Cormont, M. et al. Expression of a prenylation-deficient Rab4 inhibits the GLUT4 translocation induced by active phosphatidylinositol 3-kinase and protein kinase B. *Biochem. J.* **356** (Pt 1), 143–149 (2001).
43. Kowluru, A. Protein prenylation in glucose-induced insulin secretion from the pancreatic islet beta cell: a perspective. *J. Cell. Mol. Med.* **12**, 164–173 (2008).
44. Asano, T. et al. The role of N-glycosylation of GLUT1 for glucose transport activity. *J. Biol. Chem.* **266**, 24632–24636 (1991).
45. Buchakjian, M.R. & Kornbluth, S. The engine driving the ship: metabolic steering of cell proliferation and death. *Nat. Rev. Mol. Cell Biol.* **11**, 715–727 (2010).
46. Fujiwara, D. et al. Statins induce apoptosis through inhibition of Ras signaling pathways and enhancement of Bim and p27 expression in human hematopoietic tumor cells. *Tumour Biol.* **39**, 1010428317734947 (2017).
47. Ung, M.H. et al. Statins associate with improved mortality among patients with certain histological subtypes of lung cancer. *Lung Cancer* **126**, 89–96 (2018).
48. Hu, Y.B., Hu, E.D. & Fu, R.Q. Statin use and cancer incidence in patients with type 2 diabetes mellitus: a network meta-analysis. *Gastroenterol. Res. Pract.* **2018**, 8620682 (2018).

© 2020 The Authors. *Clinical and Translational Science* published by Wiley Periodicals, Inc. on behalf of the American Society for Clinical Pharmacology and Therapeutics. This is an open access article under the terms of the Creative Commons Attribution-NonCommercial License, which permits use, distribution and reproduction in any medium, provided the original work is properly cited and is not used for commercial purposes.